Nonlinear Analysis: Modelling and Control, Vol. 31, No. 5, 1065–1088
https://doi.org/10.15388/namc.2026.31.47702

# Dynamical analysis of a fractional-order delayed predator–prey system with infected prey*

**Wei Zheng** [1], **Jimin Zhang**

School of Mathematics and Statistics, Heilongjiang University,
Harbin 150080, China

Heilongjiang Provincial Key Laboratory of the Theory
and Computation of Complex Systems,
Harbin 150080, Heilongjiang, China

weizheng@hlju.edu.cn; zhangjm1978@hotmail.com

**Received:** December 15, 2025 / **Revised:** April 26, 2026 / **Published online:** July 10, 2026

**Abstract.** This paper investigates the dynamics and control of a fractional-order delayed predator–prey system with disease in the prey. The existence conditions for all feasible equilibria are analyzed. The local asymptotic stability of these equilibria is then studied by deriving the characteristic equation and establishing the corresponding stability criterion. Furthermore, it is demonstrated that the system undergoes a Hopf bifurcation as the time delay crosses a critical threshold, leading to the emergence of sustained periodic oscillations. To suppress oscillations and control disease transmission, a time-delayed feedback controller is incorporated into the infected prey dynamics. Theoretical analysis reveals that the additional control delay can elevate the critical threshold. Numerical simulations validate this strategy, highlighting its potential for ecological management.

**Keywords:** fractional-order eco-epidemiological model, time delay, stability, Hopf bifurcation, feedback control.

## 1 Introduction

Eco-epidemiology is an emerging interdisciplinary field integrating ecology and epidemiology. It aims to understand disease transmission dynamics within populations and its subsequent effects on species composition and energy flow in ecosystems [2, 3, 25, 27]. Recent studies [10, 13, 15] have revealed that diseases not only act as key regulators of population sizes but can also significantly alter the strength of predator–prey interactions, triggering drastic oscillations in population abundances. Such disease-mediated

*This research was supported in part by the Fundamental Research Funds for Heilongjiang Provincial Universities of China (No. 2025-KYYWF-ZR0376), the National Natural Science Foundation of China (No. 12271144), and the Heilongjiang Provincial Natural Science Foundation of China (No. PL2024A009).

[1]Corresponding author.

ecological disturbances pose increasingly severe challenges to biodiversity conservation, sustainable natural resource management, and public health security.

Time delays, which are inherent to biological processes like pathogen incubation and predator digestion, play a critical role in eco-epidemiological systems. By frequently inducing oscillatory dynamics or outright destabilization, they profoundly influence fundamental outcomes such as species coexistence and extinction thresholds [9, 28]. For instance, a predator–prey model with disease spreading in the prey population and a gestation delay in predator response has been proposed [5, 21]. In such models, the delay in predator recruitment typically depends on past consumption of both susceptible and infected prey. Analyses show that introducing a delay into the predation process results in substantially more complex behavior in epidemic systems, often altering stability and promoting sustained oscillations.

Classical integer-order dynamic models, though fundamental in biological studies, are inherently limited in capturing memory effects prevalent in nature, such as the influence of infection history or population state dependence on past trajectories. Against this backdrop, fractional-order derivatives, due to their definition relying on the entire historical state of the system, can more accurately describe complex phenomena involving historical dependence and long-range correlations, such as the growth of biological individuals and the spread of diseases [8,17,19,24]. For instance, modeling studies on the global COVID-19 pandemic conducted by Xu et al. [22, 23] have shown that, compared with traditional integer-order models, models based on Caputo fractional-order derivatives significantly improve the fitting accuracy and predictive ability for transmission trends. An increasing number of empirical advantages have opened up new avenues for constructing eco-epidemiological models that are closer to reality, and also promoted the development of research on fractional-order eco-epidemiological models [4, 7, 11, 16].

Meanwhile, integrating time-delay factors into the fractional calculus framework to construct time-delayed fractional-order eco-epidemiological models holds dual significance. Firstly, it represents a necessary breakthrough beyond the limitations of traditional integer-order models and a deepening of relevant theories. Secondly, it serves as a key scientific tool that can provide in-depth insights into the nonlinear dynamics of complex biological interaction networks, reveal their stability and bifurcation behaviors, and accurately evaluate the effectiveness of intervention measures [14, 18, 26]. However, there are still significant gaps in current research on such time-delayed fractional-order eco-epidemiological models.

This paper provides a qualitative analysis of a fractional-order eco-epidemiological model with time delay. By incorporating a time-delayed feedback controller, it investigates the controller's impact on system stability and Hopf bifurcation, establishing a theoretical basis for controlling population oscillations and mitigating disease transmission. The paper is structured as follows. Section 2 presents the fractional-order delayed model, analyzes the existence conditions of all equilibria, and proves solution nonnegativity and boundedness. Section 3 analyzes the uncontrolled system, including stability and Hopf bifurcation conditions, and examines the delayed feedback controller's effect on bifurcation behavior. Section 4 presents numerical simulations validating the theoretical results. Section 5 concludes with a summary and future research directions.

## 2 Model and preliminary results

This section presents the foundation for our analysis by introducing the fractional-order dynamical model with its assumptions and the necessary mathematical preliminaries. Key lemmas on stability and bifurcation are provided, which are crucial for the subsequent dynamical analysis.

### 2.1 Model description

We consider the following fractional-order model in which a disease spreads within the prey population, while the predator remains unaffected by the disease:

$$\begin{aligned}
{}^{C}D_t^{\alpha} S(t) &= \hat{a}^{\alpha} S\left(1 - \frac{S+I}{\hat{K}}\right) - \hat{b}^{\alpha}\hat{\beta} SI - \frac{\hat{p}_1^{\alpha} SY}{1 + \hat{m}^{\alpha}\hat{p}_1^{\alpha} S + \hat{m}^{\alpha}\hat{p}_2^{\alpha} I},\\
{}^{C}Dt^{\alpha} I(t) &= \hat{b}^{\alpha}\hat{\beta} SI - \hat{c}^{\alpha} I - \frac{\hat{p}_2^{\alpha} IY}{1 + \hat{m}^{\alpha}\hat{p}_1^{\alpha} S + \hat{m}^{\alpha}\hat{p}_2^{\alpha} I},\\
{}^{C}Dt^{\alpha} Y(t) &= \frac{q(\hat{p}_1^{\alpha} S(t-\hat{\tau}) + \hat{p}_2^{\alpha} I(t-\hat{\tau}))Y(t-\hat{\tau})}{1 + \hat{m}^{\alpha}\hat{p}_1^{\alpha} S(t-\hat{\tau}) + \hat{m}^{\alpha}\hat{p}_2^{\alpha} I(t-\hat{\tau})} - \hat{d}^{\alpha} Y.
\end{aligned} \tag{1}$$

Here ${}^{C}D_t^{\alpha}$ is the $\alpha$-order Caputo derivative with $0 < \alpha \leqslant 1$, defined as

$$ {}^{C}D_t^{\alpha} f(t) = \frac{1}{\Gamma(1-\alpha)} \int_0^t \frac{f'(\tau)}{(t-\tau)^{\alpha}}\, \mathrm{d}\tau. $$

The specific biological meanings and dimensions of each variable and parameter in the model are shown in Table 1. Assuming that predators exhibit a higher predation efficiency on infected prey and adopt a Holling type II functional response for both types with

**Table 1.** Model variables and parameters with biological meanings and units.

| Variables and parameters | Meaning | Units |
|---|---|---|
| $t$ | Time | day |
| $S$ | Density of susceptible prey | individuals |
| $I$ | Density of infected prey | individuals |
| $Y$ | Density of predators | individuals |
| $\hat{a}$ | Intrinsic birth rate of susceptible prey | day$^{-1}$ |
| $\hat{K}$ | Environmental carrying capacity of prey | individuals |
| $\hat{b}$ | Infected prey contact rate | day$^{-1}$ |
| $\hat{\beta}$ | Disease transmission coefficient | individuals$^{-1}$ |
| $\hat{c}$ | Disease-induced mortality rate of infected prey | day$^{-1}$ |
| $\hat{p}1$ | Predation rate on susceptible prey | individuals$^{-1}$ day$^{-1}$ |
| $\hat{p}2$ | Predation rate on infected prey | individuals$^{-1}$ day$^{-1}$ |
| $\hat{m}$ | Handling time coefficient in Holling-II response | day |
| $q$ | Conversion efficiency of prey biomass to predators | dimensionless |
| $\hat{d}$ | Natural mortality rate of predators | day$^{-1}$ |
| $\hat{\tau}$ | Predator gestation delay | day |

a shared handling time coefficient $m$, we set the capture rates as $p_2 > p_1$. All parameters are positive.

The initial conditions take the form

$$S(\theta) = \phi_1(\theta) \geqslant 0, \quad I(\theta) = \phi_2(\theta) \geqslant 0, \quad Y(\theta) = \phi_3(\theta) \geqslant 0, \quad \theta \in [-\tau, 0].$$

Under standard results for fractional-order delay differential equations [6, 23], model (1) admits a unique solution for any initial value $(S_0, I_0, Y_0) \in \mathbb{R}^3_+$. For notational convenience, we define:

$$a = \hat{a}^\alpha, \quad b = \hat{b}^\alpha \hat{\beta}, \quad m = \hat{m}^\alpha, \quad p_1 = \hat{p}_1^\alpha, \quad p_2 = \hat{p}_2^\alpha, \quad c = \hat{c}^\alpha, \quad d = \hat{d}^\alpha.$$

In this context, the original system can be represented as follows:

$$\begin{aligned}
{}^C D_t^\alpha S(t) &= aS\left(1 - \frac{S+I}{K}\right) - bSI - \frac{p_1 SY}{1 + mp_1 S + mp_2 I}, \\
{}^C D_t^\alpha I(t) &= bSI - cI - \frac{p_2 IY}{1 + mp_1 S + mp_2 I}, \\
{}^C D_t^\alpha Y(t) &= \frac{q(p_1 S(t-\tau) + p_2 I(t-\tau))Y(t-\tau)}{1 + mp_1 S(t-\tau) + mp_2 I(t-\tau)} - dY.
\end{aligned} \tag{2}$$

## 2.2 Existence of equilibria

System (2) always admits two trivial equilibria: the extinction equilibrium $E_0(0,0,0)$ and the single-species equilibrium $E_1(K,0,0)$ in which only the susceptible prey persists at the environmental carrying capacity. Furthermore, a predator-free equilibrium $E_2(S_2, I_2, 0)$ exists, provided that $bK > c$ with the following components:

$$S_2 = \frac{c}{b}, \qquad I_2 = \frac{a(K - S_2)}{a + bK}.$$

This establishes a basic reproduction number $R_0 = bK/c > 1$, which allows the infected prey population to persist. Additionally, the system admits a disease-free equilibrium $E_3(S_3, 0, Y_3)$, where

$$S_3 = \frac{d}{p_1(q - dm)}, \qquad Y_3 = \frac{aq}{d} S_3\left(1 - \frac{S_3}{K}\right),$$

provided that $Kp_1(q - dm) > d$ holds. This condition ensures that the maximum per capita growth rate of predator exceeds the mortality rate. The existence of the endemic equilibrium $E^*(S^*, I^*, Y^*)$, where the disease persists in the predator–prey system, requires that the system

$$\begin{aligned}
&a\left(1 - \frac{S^* + I^*}{K}\right) - bI^* - \frac{p_1 Y^*}{1 + mp_1 S^* + mp_2 I^*} = 0, \\
&bS^* - c - \frac{p_2 Y^*}{1 + mp_1 S^* + mp_2 I^*} = 0, \\
&\frac{q(p_1 S^* + p_2 I^*)}{1 + mp_1 S^* + mp_2 I^*} - d = 0
\end{aligned}$$

admits a positive solution. Solving the equations, we obtain

$$S^* = \frac{K(ap_2 + cp_1) - \frac{d(a+bK)}{q-dm}}{a(p_2 - p_1)}, \qquad I^* = \frac{1}{p_2}\left(\frac{d}{q - dm} - p_1 S^*\right),$$
$$Y^* = \frac{q(bS^* - c)}{p_2(q - dm)}.$$

The endemic equilibrium $E^*$ exists under the following condition:

$$\text{(H1)} \qquad \frac{d}{p_1(q - dm)} > \frac{K(ap_2 + cp_1) - \frac{d(a+bK)}{q-dm}}{a(p_2 - p_1)} > \frac{c}{b}.$$

### 2.3 Nonnegativity and boundedness of solutions

To ensure the biological plausibility of (2), we first demonstrate that its solutions remain nonnegative and bounded for all future time.

**Lemma 1.** *Given nonnegative initial conditions*

$$S(\theta) = \phi_1(\theta) \geqslant 0, \quad I(\theta) = \phi_2(\theta) \geqslant 0, \quad Y(\theta) = \phi_3(\theta) \geqslant 0, \quad \theta \in [-\tau, 0],$$

*the solutions* $(S(t), I(t), Y(t))$ *of* (2) *remain nonnegative for all* $t > 0$.

*Proof.* Suppose there exists $t_1 > 0$ such that $S(t_1) < 0$. Since $S(t)$ is continuous and $S(0) \geqslant 0$, there exists a first point $t_0 = \inf\{t > 0\colon\ S(t) < 0\}$ satisfying

$$S(t_0) = 0, \quad S(t) < 0 \quad \text{for } t \in (t_0,\, t_0 + \epsilon),\ \epsilon > 0.$$

Evaluating the first equation of (2) at $t = t_0$ yields ${}^C D_t^\alpha S(t_0) = 0$. According to the definition of the Caputo derivative, $S(t)$ remains identically zero in a neighborhood of $t_0$ due to the uniqueness of solutions. This contradicts the assumption that $S(t) < 0$ immediately after $t_0$. Hence, $S(t) \geqslant 0$ for all $t \geqslant 0$. The same argument yields $I(t) \geqslant 0$.

Now suppose $Y(t_1) < 0$ for some $t_1 > 0$, and let $t_0 = \inf\{t > 0\colon\ Y(t) < 0\}$. Then $Y(t_0) = 0$. Substituting into the third equation gives

$${}^C D_t^\alpha Y(t_0) = \frac{q(p_1 S(t_0 - \tau) + p_2 I(t_0 - \tau))Y(t_0 - \tau)}{1 + mp_1 S(t_0 - \tau) + mp_2 I(t_0 - \tau)} - dY(t_0).$$

Since $S(t_0 - \tau), I(t_0 - \tau) \geqslant 0$ (by the initial conditions on $[-\tau, 0]$) and $Y(t_0 - \tau) \geqslant 0$, the first term is nonnegative. However, because $Y(t_0 - \tau) \geqslant 0$, if $Y(t_0 - \tau) > 0$, then the right-hand side would be positive, contradicting ${}^C D_t^\alpha Y(t_0) = 0$. Hence, we must have $Y(t_0 - \tau) = 0$. Repeated application of this argument backward in time shows that $Y(t)$ vanishes identically on $[t_0 - \tau,\, t_0]$. By the uniqueness of solutions, $Y(t)$ remains zero for $t > t_0$, which contradicts the assumption that $Y(t)$ becomes negative. Consequently, $Y(t) \geqslant 0$ for all $t \geqslant 0$.

Thus, all three populations remain nonnegative for all time under nonnegative initial conditions. $\square$

**Lemma 2.** *The solutions of system* (2) *are uniformly bounded.*

*Proof.* Define the total prey population $N(t) = S(t) + I(t)$. Adding the first two equations of (2) we obtain

$$^{C}D_t^{\alpha}N(t) = aS\left(1 - \frac{N}{K}\right) - cI - \frac{(p_1S + p_2I)Y}{1 + mp_1S + mp_2I} \leqslant aS\left(1 - \frac{N}{K}\right).$$

Observe that $^{C}D_t^{\alpha}N(t) \leqslant 0$ when $N(t) > K$. We now prove that $N(t) \leqslant \max\{N(0), K\}$ for all $t \geqslant 0$. Suppose for contradiction that $N(t_1) > \max\{N(0), K\}$ for some $t_1 > 0$. Let $t_0 = \sup\{t < t_1\colon N(t) \leqslant \max\{N(0), K\}\}$. Then $N(t_0) = \max\{N(0), K\}$ and $N(t) > K$ on $(t_0, t_1]$, which implies $^{C}D_t^{\alpha}N(t) \leqslant 0$, $t \in (t_0, t_1]$. By the integral representation of the Caputo derivative, we obtain $N(t_1) \leqslant N(t_0)$, which is a contradiction. Therefore $N(t)$ is uniformly bounded.

Now we establish boundedness of the predator population $Y(t)$. From the third equation of (2),

$$^{C}D_t^{\alpha}Y(t) \leqslant \frac{q(p_1S + p_2I)}{1 + mp_1S + mp_2I}Y(t - \tau) \leqslant q\frac{p_2N}{1 + mp_1N}Y(t - \tau).$$

Since $N(t)$ is bounded, there exists a constant $\eta > 0$ such that

$$^{C}D_t^{\alpha}Y(t) \leqslant \eta Y(t - \tau).$$

Then $Y(t)$ is bounded on any finite interval. Moreover, using the method of steps and the boundedness of $N(t)$, one can show that $Y(t)$ remains uniformly bounded for all $t \geqslant 0$. □

### 2.4 Preliminaries on stability

For the purpose of analyzing the local stability of the equilibria, we first introduce the following lemmas regarding the stability of fractional differential equations.

**Lemma 3.** (*See* [12].) *Consider the fractional-order system*

$$^{C}D_t^{\alpha}x(t) = f\bigl(t, x(t)\bigr),$$
$$x(0) = x_0$$

*with* $\alpha \in (0, 1]$ *and* $f(t, x(t)) : \mathbb{R}^+ \times \mathbb{R}^n \to \mathbb{R}^n$. *The equilibrium is locally asymptotically stable if all roots* $s_j$ $(j = 1, 2, \dots, N)$ *of the characteristic equation* $\det(s^{\alpha}I - J) = 0$ *satisfy* $|\arg(s_j)| > \pi/2$, *where* $J = \partial f(t, x)/\partial x$ *is evaluated at the equilibrium. It is unstable if there is a root such that* $|\arg(s)| < \pi/2$.

**Remark 1.** According to Lemma 3, the equilibrium is locally asymptotically stable, provided the characteristic roots satisfy $|\arg(s)| > \pi/2$, a condition equivalent to $|\arg(s^{\alpha})| > \alpha\pi/2$. It follows that the stability criterion is more easily satisfied as $\alpha$ approaches 0.

**Lemma 4.** (*See* [20].) *Consider a $n$-dimensional fractional-order system with delay*

$$ {}^{C}D_t^{\alpha} x_i(t) = g_i(x_1, x_2, \ldots, x_n, \tau), \quad i = 1, 2, \ldots, n, \tag{3} $$

*where $\alpha \in (0,1]$, and the time delay $\tau \geqslant 0$. It will undergo a Hopf bifurcation at the equilibrium $x^* = (x_1^*, x_2^*, \ldots, x_n^*)*$ when $\tau = \tau_0$ if following conditions are satisfied*:

(i) *All the eigenvalues of the coefficient matrix of the linearized system of* (3) *satisfy* $|\arg(s^{\alpha})| > \alpha\pi/2$.
(ii) *The characteristic equation of* (3) *has purely imaginary roots* $\pm \mathrm{i}\varphi_0$ *when* $\tau = \tau_0$.
(iii) $\mathrm{d}\,\mathrm{Re}[s(\tau)]/\mathrm{d}\tau|_{\tau=\tau_0} > 0$, *where* $\mathrm{Re}[\cdot]$ *denotes the real part of a complex number.*

## 3 Stability and bifurcation analysis

We first linearize system (2) around an arbitrary equilibrium point $\hat{E} = (\hat{S}, \hat{I}, \hat{Y})$, yielding

$$ \begin{aligned} {}^{C}D_t^{\alpha} S(t) &= a_{11}S - a_{12}I - a_{13}Y + c_1, \\ {}^{C}D_t^{\alpha} I(t) &= a_{21}S + a_{22}I - a_{23}Y + c_2, \\ {}^{C}D_t^{\alpha} Y(t) &= a_{31}S(t-\tau) + a_{32}I(t-\tau) + a_{33}Y(t-\tau) - dY + c_3. \end{aligned} \tag{4} $$

The coefficients of the Jacobian matrix are given by

$$ a_{11} = a\left(1 - \frac{2\hat{S} + \hat{I}}{K}\right) - b\hat{I} - \frac{p_1\hat{Y}(1 + mp_2\hat{I})}{(1 + mp_1\hat{S} + mp_2\hat{I})^2}, \qquad a_{13} = \frac{p_1\hat{S}}{1 + mp_1\hat{S} + mp_2\hat{I}}, $$

$$ a_{12} = \left(\frac{a}{K} + b\right)\hat{S} + \frac{mp_1p_2\hat{S}\hat{Y}}{(1 + mp_1\hat{S} + mp_2\hat{I})^2}, \qquad a_{21} = b\hat{I} + \frac{mp_1p_2\hat{I}\hat{Y}}{(1 + mp_1\hat{S} + mp_2\hat{I})^2}, $$

$$ a_{22} = b\hat{S} - c - \frac{p_2\hat{Y}(1 + mp_1\hat{S})}{(1 + mp_1\hat{S} + mp_2\hat{I})^2}, \qquad a_{23} = \frac{p_2\hat{I}}{1 + mp_1\hat{S} + mp_2\hat{I}}, $$

$$ a_{31} = \frac{qp_1\hat{Y}}{(1 + mp_1\hat{S} + mp_2\hat{I})^2}, \qquad a_{32} = \frac{qp_2\hat{Y}}{(1 + mp_1\hat{S} + mp_2\hat{I})^2}, $$

$$ a_{33} = \frac{q(p_1\hat{S} + p_2\hat{I})}{1 + mp_1\hat{S} + mp_2\hat{I}}, \qquad c_1 = -a_{11}\hat{S} + a_{12}\hat{I} + a_{13}\hat{Y}, $$

$$ c_2 = -a_{21}\hat{S} - a_{22}\hat{I} + a_{23}\hat{Y}, \qquad c_3 = -a_{31}\hat{S} - a_{32}\hat{I} - (a_{33} - d)\hat{Y}. $$

Applying the Laplace transform to (4), we obtain the characteristic matrix

$$ \varDelta(s) = \begin{pmatrix} s^{\alpha} - a_{11} & a_{12} & a_{13} \\ -a_{21} & s^{\alpha} - a_{22} & a_{23} \\ -a_{31}\mathrm{e}^{-s\tau} & -a_{32}\mathrm{e}^{-s\tau} & s^{\alpha} - a_{33}\mathrm{e}^{-s\tau} + d \end{pmatrix}. $$

Then the characteristic equation of the system is given by

$$ \left|\varDelta(s)\right| = Q_1(s) - Q_2(s)\mathrm{e}^{-s\tau} = 0, \tag{5} $$

where

$$\begin{aligned}
Q_1(s) &= s^{3\alpha} + (d - a_{11} - a_{22})s^{2\alpha} + (a_{11}a_{22} + a_{12}a_{21} - a_{11}d - a_{22}d)s^{\alpha} \\
&\quad + a_{11}a_{22}d + a_{12}a_{21}d, \\
Q_2(s) &= a_{33}s^{2\alpha} - (a_{11}a_{33} + a_{13}a_{31} + a_{22}a_{33} + a_{23}a_{32})s^{\alpha} + a_{11}a_{22}a_{33} \\
&\quad + a_{12}a_{21}a_{33} + a_{11}a_{23}a_{32} + a_{12}a_{23}a_{31} - a_{13}a_{21}a_{32} + a_{13}a_{22}a_{31}.
\end{aligned}$$

### 3.1 Stability analysis

We now analyze the stability of each equilibrium point for the case $\tau = 0$ by examining the roots of their respective characteristic equations.

The characteristic equation at $E_0$ is

$$\bigl(s^{\alpha} - a\bigr)\bigl(s^{\alpha} + c\bigr)\bigl(s^{\alpha} + d\bigr) = 0.$$

It clearly has a positive real root, therefore $E_0$ is always unstable.

The characteristic equation at $E_1$ is

$$\bigl(s^{\alpha} + a\bigr)\bigl(s^{\alpha} - bK + c\bigr)\left(s^{\alpha} - \frac{Kp_1q}{1 + Kmp_1} + d\right) = 0.$$

Then $E_1$ is locally asymptotically stable, provided that

$$bK < c \quad \text{and} \quad Kp_1(q - dm) < d. \tag{6}$$

If either condition is violated, then $E_1$ is unstable, indicating the potential existence of $E_2$ or $E_3$.

The characteristic equation at $E_2$ is

$$\left(s^{2\alpha} + \frac{ac}{bK}s^{\alpha} + \frac{ac(bK - c)}{bK}\right)\left(s^{\alpha} + d - \frac{q(p_1S_2 + p_2I_2)}{1 + mp_1S_2 + mp_2I_2}\right) = 0.$$

Since $bK - c > 0$, the quadratic factor yields two roots, which are negative roots or conjugate complex roots with negative real parts. Thus, $E_2$ is locally asymptotically stable if

$$(q - dm)(p_1S_2 + p_2I_2) < d,$$

that is,

$$(q - dm)\left(cp_1 + \frac{ap_2(bK - c)}{a + bK}\right) < d. \tag{7}$$

The characteristic equation at $E_3$ has one root

$$s^{\alpha} = bS_3 - c - \frac{ap_2(K - S_3)}{p_1K},$$

which is negative if $p_1K(bS_3 - c) - ap_2(K - S_3) < 0$. The other two roots satisfy

$$s^{2\alpha} + \frac{a(dm + q)S_3 - adKm}{Kq}s^{\alpha} + \frac{ad(q - dm)(K - S_3)}{Kq} = 0.$$

They have nonpositive real parts when $(dm+q)S_3 \geqslant dKm$. If $(dm+q)S_3 < dKm$, then $|\arg(s^\alpha)|| > \alpha\pi/2$, provided that

$$\frac{\sqrt{4adKq(q-dm)(K-S_3)-(a(dm+q)S_3-adKm)^2}}{adKm-a(dm+q)S_3} > \tan\frac{\alpha\pi}{2}. \tag{8}$$

The characteristic equation at $E^*$ is

$$z^3 + A_2 z^2 + A_1 z + \frac{p_2(q-dm)S^* I^* Y^* A_0}{A^2} = 0,$$

where

$$z = s^\alpha, \qquad A = \frac{q}{q-dm}, \qquad A_0 = \frac{a(p_2-p_1)}{K} - \frac{2mp_1^2 p_2 Y^*}{A^2},$$

$$A_1 = \frac{mp_2 S^* I^* Y^*(2bp_1 - A_0)}{A^2} + \frac{Y^*(q-dm)(p_1^2 S^* + p_2^2 I^*)}{A^2} + bS^* I^*\left(\frac{a}{K} + b\right),$$

$$A_2 = \frac{aS^*}{K} - \frac{mY^*(p_1^2 S^* + p_2^2 I^*)}{A^2}.$$

Three roots can be expressed as

$$z_k = \omega^k \sqrt[3]{\frac{-B_2}{2} + \sqrt{\frac{B_2^2}{4} + \frac{B_1^3}{27}}} + \omega^{3-k} \sqrt[3]{\frac{-B_2}{2} - \sqrt{\frac{B_2^2}{4} + \frac{B_1^3}{27}}} - \frac{A_2}{3}, \tag{9}$$

$k = 0, 1, 2$. Here

$$\omega = -\frac{1}{2} + \mathrm{i}\frac{\sqrt{3}}{2}, \qquad B_1 = A_1 - \frac{{A_2}^2}{3},$$

$$B_2 = \frac{2{A_2}^3}{27} - \frac{A_1 A_2}{3} + \frac{p_2(q-dm)S^* I^* Y^* A_0}{A^2}.$$

Then the condition for the local asymptotic stability of $E^*$ is

(H2) $|\arg(z_k)| > \alpha\pi/2$ for $k = 0, 1, 2$.

Based on the linearization analysis and characteristic equations derived above, we now summarize the local stability conditions for all equilibria of system (2) in the absence of time delay.

**Theorem 1.** *For system* (2) *with* $\tau = 0$, *the local stability of equilibria is characterized as follows*:

(i) $E_0(0,0,0)$ *is always unstable.*
(ii) $E_1(K,0,0)$ *is locally asymptotically stable if* (6) *holds.*
(iii) $E_2(S_2, I_2, 0)$ *is locally asymptotically stable if* (7) *holds.*
(iv) $E_3(S_3, 0, Y_3)$ *is locally asymptotically stable if* $bS_3 - p_2 Y_3 - c < 0$, *and either* $S_3 \geqslant dKm/(dm+q)$ *or* (8) *holds.*
(v) $E^*(S^*, I^*, Y^*)$ *is locally asymptotically stable if* (H2) *holds.*

### 3.2 Hopf bifurcation Analysis

We now derive the conditions under which the endemic equilibrium $E^*$ undergoes a Hopf bifurcation as the time delay $\tau > 0$ varies. The characteristic equation (5) at $E^*$ is expressed as

$$Q_1^*(s) - Q_2^*(s)\mathrm{e}^{-s\tau} = 0, \tag{10}$$

where

$$\begin{aligned}
Q_1^*(s) &= s^{3\alpha} + (d + A_2)s^{2\alpha} + (dA_2 + C_0)s^{\alpha} + dC_0,\\
Q_2^*(s) &= ds^{2\alpha} + C_1 s^{\alpha} + dC_0 - \frac{p_2(q - dm)S^*I^*Y^*A_0}{A^2},\\
C_0 &= \frac{mp_2S^*I^*Y^*}{A^2}(2bp_1 - A_0) + bS^*I^*\left(\frac{a}{K} + b\right),\\
C_1 &= \frac{adS^*}{K} - \frac{qY^*}{A^2}\left(p_1^2 S^* + p_2^2 I^*\right).
\end{aligned}$$

Substituting $s = \mathrm{i}\varphi = \varphi\mathrm{e}^{\pi\mathrm{i}/2}(\varphi > 0)$ into Eq. (10) and separating the real and imaginary parts yields

$$\begin{aligned}
\cos(\varphi\tau) &= \frac{\mathrm{Re}[Q_1^*(\mathrm{i}\varphi)]\,\mathrm{Re}[Q_2^*(\mathrm{i}\varphi)] + \mathrm{Im}[Q_1^*(\mathrm{i}\varphi)]\,\mathrm{Im}[Q_2^*(\mathrm{i}\varphi)]}{\mathrm{Re}^2[Q_2^*(\mathrm{i}\varphi)] + \mathrm{Im}^2[Q_2^*(\mathrm{i}\varphi)]} := f_1(\varphi),\\
\sin(\varphi\tau) &= \frac{\mathrm{Re}[Q_1^*(\mathrm{i}\varphi)]\,\mathrm{Im}[Q_2^*(\mathrm{i}\varphi)] - \mathrm{Im}[Q_1^*(\mathrm{i}\varphi)]\,\mathrm{Re}[Q_2^*(\mathrm{i}\varphi)]}{\mathrm{Re}^2[Q_2^*(\mathrm{i}\varphi)] + \mathrm{Im}^2[Q_2^*(\mathrm{i}\varphi)]} := f_2(\varphi).
\end{aligned} \tag{11}$$

Here the real and imaginary parts are given by

$$\begin{aligned}
\mathrm{Re}\big[Q_1^*(\mathrm{i}\varphi)\big] &= \varphi^{3\alpha}\cos\frac{3\alpha\pi}{2} + (d + A_2)\varphi^{2\alpha}\cos(\alpha\pi) + (dA_2 + C_0)\varphi^{\alpha}\cos\frac{\alpha\pi}{2} + dC_0,\\
\mathrm{Im}\big[Q_1^*(\mathrm{i}\varphi)\big] &= \varphi^{3\alpha}\sin\frac{3\alpha\pi}{2} + (d + A_2)\varphi^{2\alpha}\sin(\alpha\pi) + (dA_2 + C_0)\varphi^{\alpha}\sin\frac{\alpha\pi}{2},\\
\mathrm{Re}\big[Q_2^*(\mathrm{i}\varphi)\big] &= d\varphi^{2\alpha}\cos(\alpha\pi) + C_1\varphi^{\alpha}\cos\frac{\alpha\pi}{2} + dC_0 - \frac{p_2(q - dm)S^*I^*Y^*A_0}{A^2},\\
\mathrm{Im}\big[Q_2^*(\mathrm{i}\varphi)\big] &= d\varphi^{2\alpha}\sin(\alpha\pi) + C_1\varphi^{\alpha}\sin\frac{\alpha\pi}{2}.
\end{aligned}$$

Assume that Eq. (11) admits a positive real root $\varphi_0$. Then the critical values of time delay $\tau$ are given by

$$\tau_0^{(k)} = \frac{1}{\varphi_0}\big(\arccos f_1(\varphi_0) + 2k\pi\big) = \frac{1}{\varphi_0}\big(\arcsin f_2(\varphi_0) + 2k\pi\big), \tag{12}$$

where $k = 0, 1, 2 \dots$. Let $\tau_0 = \tau_0^{(0)}$. Next, differentiating both sides of Eq. (10) with respect to $\tau$ and simplifying yields

$$\left(\frac{\mathrm{d}s}{\mathrm{d}\tau}\right)^{-1} = \frac{Q_2^{*'}(s) - Q_1^{*'}(s)\mathrm{e}^{s\tau}}{sQ_2^*(s)} - \frac{\tau}{s},$$

where

$$Q_1^{*'}(s) = 3\alpha s^{3\alpha-1} + 2\alpha(d + A_2)s^{2\alpha-1} + \alpha(dA_2 + C_0)s^{\alpha-1},$$
$$Q_2^{*'}(s) = 2\alpha d s^{2\alpha-1} + \alpha C_1 s^{\alpha-1}.$$

Substituting $s = \mathrm{i}\varphi_0$ and $\tau = \tau_0$, we obtain

$$\operatorname{Re}\left[\left(\frac{\mathrm{d}s}{\mathrm{d}\tau}\right)^{-1}\right]_{\tau=\tau_0} = -\frac{M_1N_1 + M_2N_2}{\varphi_0(N_1^2 + N_2^2)}$$

in which

$$M_1 = \operatorname{Re}\bigl[Q_2^{*'}(\mathrm{i}\varphi_0)\bigr] - \operatorname{Re}\bigl[Q_1^{*'}(\mathrm{i}\varphi_0)\bigr]\cos(\varphi_0\tau_0) + \operatorname{Im}\bigl[Q_1^{*'}(\mathrm{i}\varphi_0)\bigr]\sin(\varphi_0\tau_0),$$
$$M_2 = \operatorname{Im}\bigl[Q_2^{*'}(\mathrm{i}\varphi_0)\bigr] - \operatorname{Im}\bigl[Q_1^{*'}(\mathrm{i}\varphi_0)\bigr]\cos(\varphi_0\tau_0) - \operatorname{Re}\bigl[Q_1^{*'}(\mathrm{i}\varphi_0)\bigr]\sin(\varphi_0\tau_0),$$
$$N_1 = \operatorname{Im}\bigl[Q_2^{*}(\mathrm{i}\varphi_0)\bigr],$$
$$N_2 = -\operatorname{Re}\bigl[Q_2^{*}(\mathrm{i}\varphi_0)\bigr].$$

Therefore, if the condition

(H3) $M_1N_1 + M_2N_2 < 0$

is satisfied, then $\operatorname{Re}[(\mathrm{d}s/\mathrm{d}\tau)^{-1}]_{\tau=\tau_0} > 0$. According to Lemma 4, a Hopf bifurcation occurs at the equilibrium $E^*$ when $\tau = \tau_0$.

**Theorem 2.** *Assume that conditions* (H1) *and* (H2) *hold. If a positive root $\varphi_0$ of the characteristic equation* (11) *exists, leading to a critical delay $\tau_0$, and condition* (H3) *is satisfied, then system* (4) *undergoes a Hopf bifurcation at $E^*$ when $\tau = \tau_0$.*

**Remark 2.** Equation (11) is a transcendental equation that may admit multiple positive real roots $\varphi_0, \varphi_1, \dots, \varphi_n$ ($n \geqslant 1$). Each positive root $\varphi_i$ corresponds to a sequence of critical delays given by (12). The phenomenon of stability switches—where the stability of $E^*$ alternates as $\tau$ increases—occurs if the sign of $\operatorname{Re}[(\mathrm{d}s/\mathrm{d}\tau)^{-1}]$ alternates at consecutive critical delays. The specific switching pattern is determined numerically in Section 4.

### 3.3 Bifurcation control via time-delayed feedback

Given the inherent complexity of eco-epidemiological systems, effective control strategies are crucial for guiding them toward desirable outcomes. These strategies include vaccination, habitat management, and population regulation, and are aimed at achieving goals such as population coexistence, disease eradication, and sustainable resource use. These efforts are vital for advancing biodiversity conservation, maintaining ecosystem services, and protecting public health. To control disease outbreaks, a time-delayed feedback controller

$$\mu(t) = h\bigl(I(t) - I(t - v)\bigr)$$

is introduced into the infected prey equation, resulting in the controlled system

$$
\begin{aligned}
{}^{C}D_t^{\alpha} S(t) &= aS\left(1 - \frac{S+I}{K}\right) - bSI - \frac{p_1 SY}{1 + mp_1 S + mp_2 I},\\
{}^{C}D_t^{\alpha} I(t) &= bSI - cI - \frac{p_2 IY}{1 + mp_1 S + mp_2 I} + \mu(t),\\
{}^{C}D_t^{\alpha} Y(t) &= \frac{q(p_1 S(t-\tau) + p_2 I(t-\tau))Y(t-\tau)}{1 + mp_1 S(t-\tau) + mp_2 I(t-\tau)} - dY.
\end{aligned}
\tag{13}
$$

Here the parameter $v$ denotes the sampling interval for infected population data, and $h(\cdot)$ represents a proportional control gain defined as $h(x) = hx$. A negative feedback gain $h < 0$ implements suppressive control measures to reduce infections. It follows directly that when $h = 0$ or $v = 0$, the dynamical system described by (13) degenerates into the original uncontrolled system (2). This implies that the controller introduces no alteration to the equilibrium points of the system.

**Remark 3.** For the controlled system (13) with $h < 0$, the nonnegativity of solutions is still preserved. Indeed, when $I(t) = 0$, the second equation yields

$$
{}^{C}D_t^{\alpha} I(t) = -hI(t-v) \geqslant 0
$$

since $h < 0$ and $I(t-v) \geqslant 0$ by the initial condition. Thus, $I(t)$ cannot cross zero to become negative. The arguments for $S(t)$ and $Y(t)$ remain the same as in the uncontrolled case. Hence, all solutions remain nonnegative for $t \geqslant 0$ under nonnegative initial conditions.

For given values of $\tau > \tau_0$ and $v > 0$, the characteristic equation corresponding to system (13) is given by

$$
Q_3(s) + hQ_4(s)\mathrm{e}^{-sv} = 0. \tag{14}
$$

Here

$$
\begin{aligned}
Q_3(s) &= Q_1(s) - Q_2(s)\mathrm{e}^{-s\tau} - hQ_4(s),\\
Q_4(s) &= \left(\frac{qp_1{}^2 S^*(bS^* - c)}{p_2 A} - \frac{adS^*}{K} - ds^{\alpha}\right)\mathrm{e}^{-s\tau}\\
&\quad + s^{2\alpha} + (d - D)s^{\alpha} - dD\\
D &= \frac{mp_1{}^2 S^*(bS^* - c)}{p_2 A} - \frac{aS^*}{K}.
\end{aligned}
$$

Substituting $s = \mathrm{i}\psi = \psi\mathrm{e}^{\pi\mathrm{i}/2}$ with $\psi > 0$ into Eq. (14) and separating the real and imaginary parts leads to

$$
\begin{aligned}
h\cos(\psi v) &= -\frac{\mathrm{Re}[Q_3(\mathrm{i}\psi)]\,\mathrm{Re}[Q_4(\mathrm{i}\psi)] + \mathrm{Im}[Q_3(\mathrm{i}\psi)]\,\mathrm{Im}[Q_4(\mathrm{i}\psi)]}{\mathrm{Re}^2[Q_4(\mathrm{i}\psi)] + \mathrm{Im}^2[Q_4(\mathrm{i}\psi)]} := g_1(\psi),\\
h\sin(\psi v) &= \frac{\mathrm{Im}[Q_3(\mathrm{i}\psi)]\,\mathrm{Re}[Q_4(\mathrm{i}\psi)] - \mathrm{Re}[Q_3(\mathrm{i}\psi)]\,\mathrm{Im}[Q_4(\mathrm{i}\psi)]}{\mathrm{Re}^2[Q_4(\mathrm{i}\psi)] + \mathrm{Im}^2[Q_4(\mathrm{i}\psi)]} := g_2(\psi),
\end{aligned}
\tag{15}
$$

where

$$\begin{aligned}
\operatorname{Re}\bigl[Q_3(\mathrm{i}\psi)\bigr] &= \operatorname{Re}\bigl[Q_1(\mathrm{i}\psi)\bigr] - \operatorname{Re}\bigl[Q_2(\mathrm{i}\psi)\bigr]\cos(\psi\tau) - \operatorname{Im}\bigl[Q_2(\mathrm{i}\psi)\bigr]\sin(\psi\tau) \\
&\quad - h\operatorname{Re}\bigl[Q_4(\mathrm{i}\psi)\bigr], \\
\operatorname{Im}\bigl[Q_3(\mathrm{i}\psi)\bigr] &= \operatorname{Im}\bigl[Q_1(\mathrm{i}\psi)\bigr] - \operatorname{Im}\bigl[Q_2(\mathrm{i}\psi)\bigr]\cos(\psi\tau) + \operatorname{Re}\bigl[A_2(\mathrm{i}\psi)\bigr]\sin(\psi\tau) \\
&\quad - h\operatorname{Im}\bigl[Q_4(\mathrm{i}\psi)\bigr], \\
\operatorname{Re}\bigl[Q_4(\mathrm{i}\psi)\bigr] &= \psi^{2\alpha}\cos(\alpha\pi) - d\psi^{\alpha}\cos\left(\psi\tau - \frac{\alpha\pi}{2}\right) + (d-D)\psi^{\alpha}\cos\frac{\alpha\pi}{2} - dD \\
&\quad + \left(\frac{q{p_1}^2S^*(bS^*-c)}{p_2A} - \frac{adS^*}{K}\right)\cos(\psi\tau), \\
\operatorname{Im}\bigl[Q_4(\mathrm{i}\psi)\bigr] &= \psi^{2\alpha}\sin(\alpha\pi) + d\psi^{\alpha}\sin\left(\psi\tau - \frac{\alpha\pi}{2}\right) + (d-D)\psi^{\alpha}\sin\frac{\alpha\pi}{2} \\
&\quad + \left(\frac{q{p_1}^2S^*(bS^*-c)}{p_2A} - \frac{adS^*}{K}\right)\sin(\psi\tau).
\end{aligned}$$

Assume that Eq. (15) possesses a positive real root $\psi_0$. Then, for $k = 0, 1, 2, \dots$, the corresponding critical values of the time delay $v$ are given by

$$v_0^{(k)} = \frac{1}{\psi_0}\left(\arccos\frac{g_1(\psi_0)}{h} + 2k\pi\right) = \frac{1}{\psi_0}\left(\arcsin\frac{g_2(\psi_0)}{h} + 2k\pi\right). \tag{16}$$

Let $v_0 = v_0^{(0)}$ denote the smallest such value. Next, differentiating (14) with respect to $v$ and simplifying yields

$$\left(\frac{\mathrm{d}s}{\mathrm{d}v}\right)^{-1} = \frac{Q_3'(s)\mathrm{e}^{sv} + hQ_4'(s)}{hsQ_4(s)} - \frac{v}{s}.$$

Here

$$\begin{aligned}
Q_3'(s) &= Q_1'(s) - Q_2'(s)\mathrm{e}^{-s\tau} + \tau Q_2(s)\mathrm{e}^{-s\tau} - hQ_4'(s), \\
Q_4'(s) &= 2\alpha s^{2\alpha-1} + \alpha(d-D)s^{\alpha-1} - \alpha d s^{\alpha-1}\mathrm{e}^{-s\tau} \\
&\quad - \tau\left(\frac{qp_1^2S^*(bS^*-c)}{p_2A} - \frac{adS^*}{K} - ds^{\alpha}\right)\mathrm{e}^{-s\tau}.
\end{aligned}$$

Substituting $s = \mathrm{i}\psi_0$ and $v = v_0$, we obtain

$$\operatorname{Re}\left[\left(\frac{\mathrm{d}s}{\mathrm{d}v}\right)^{-1}\right]_{v=v_1} = \frac{U_1V_1 + U_2V_2}{h\psi_1(V_1^2 + V_2^2)}$$

in which

$$\begin{aligned}
U_1 &= \operatorname{Re}\bigl[Q_3'(\mathrm{i}\psi_0)\bigr]\cos(\psi_0v_0) - \operatorname{Im}\bigl[Q_3'(\mathrm{i}\psi_0)\bigr]\sin(\psi_0v_0) + h\operatorname{Re}\bigl[Q_4'(\mathrm{i}\psi_0)\bigr], \\
U_2 &= \operatorname{Im}\bigl[Q_3'(\mathrm{i}\psi_0)\bigr]\cos(\psi_0v_0) + \operatorname{Re}\bigl[Q_3'(\mathrm{i}\psi_0)\bigr]\sin(\psi_0v_0) + h\operatorname{Im}\bigl[Q_4'(\mathrm{i}\psi_0)\bigr], \\
V_1 &= -\operatorname{Im}\bigl[Q_4(\mathrm{i}\psi_0)\bigr], \qquad V_2 = \operatorname{Re}\bigl[Q_4(\mathrm{i}\psi_0)\bigr].
\end{aligned}$$

Hence, if the condition

(H4) $U_1V_1 + U_2V_2 > 0$

is satisfied, it follows that $\mathrm{Re}[(\mathrm{d}s/\mathrm{d}v)^{-1}]_{v=v_0} < 0$.

**Theorem 3.** *For system* (13)*, suppose that* (H1)–(H3) *hold. If* $\tau > \tau_0$ *and* (H4) *is satisfied, then the positive equilibrium* $E^*$ *of system* (13) *undergoes a Hopf bifurcation at* $v = v_0$*, where its stability switches from unstable to stable.*

**Remark 4.** As elaborated in Remark 2, Eq. (15) is a transcendental equation that may possess multiple positive real roots. Accordingly, the phenomenon of stability switches will occur if the sign of $\mathrm{Re}[(\mathrm{d}s/\mathrm{d}v)^{-1}]$ alternates at consecutive critical delays.

## 4 Simulations

In this section, we conduct numerical simulations to validate the theoretical results on stability and bifurcation obtained in the previous sections, and to demonstrate the effectiveness of the proposed time-delayed feedback controller. All simulations are conducted using the parameter values listed in Table 2, unless otherwise specified. The initial conditions are set as $S(t) = 1.6$, $I(t) = 0.5$, and $Y(t) = 1.5$ for $t \in (-\tau, 0]$.

### 4.1 Stability and bifurcation analysis

We first consider the uncontrolled system (2) described by the fractional-order differential equations. The parameter values in Table 2 satisfy condition (H1), confirming the existence of a positive equilibrium $E^* = (1.3797, 0.8393, 1.6193)$. Further calculation yields three roots in (9): $z_0 \approx -0.002$, $z_1 \approx 0.0182 + 0.6301\mathrm{i}$, and $z_2 \approx 0.0182 - 0.6301\mathrm{i}$. Since $|\arg(z_2)| - \alpha\pi/2 = 0.0497 > 0$, condition (H2) is satisfied. When $\tau = 0$, the positive equilibrium $E^*$ of system (2) is locally asymptotically stable, and the numerical simulation results are shown in Fig. 1.

When $\tau > 0$, solving Eq. (11) yields two sets of critical parameters:

$$(\varphi_0^-, \tau_{0,0}^-) \approx (0.594039, 1.8628) \quad \text{and} \quad (\varphi_0^+, \tau_{0,0}^+) \approx (0.550496, 4.6668).$$

According to (12), these define two infinite sequences of critical delays:

$$\tau_{0,k}^{\pm} = \tau_{0,0}^{\pm} + \frac{2k\pi}{\varphi_0^{\pm}}, \quad k = 0, 1, 2, \dots .$$

The transversality condition analysis shows that $M_1N_1 + M_2N_2 \approx -0.0113 < 0$ for $(\varphi_0^-, \tau_{0,k}^-)$, and $M_1N_1 + M_2N_2 \approx 0.0092 > 0$ for $(\varphi_0^+, \tau_{0,k}^+)$. Consequently,

$$\mathrm{Re}\left[\left(\frac{\mathrm{d}s}{\mathrm{d}\tau}\right)^{-1}\right]_{\tau=\tau_{0,k}^-} > 0 \quad \text{and} \quad \mathrm{Re}\left[\left(\frac{\mathrm{d}s}{\mathrm{d}\tau}\right)^{-1}\right]_{\tau=\tau_{0,k}^+} < 0 \quad \text{for } k = 0, 1, 2, \dots .$$

The ordering of the initial critical delays is given by

$$0 < \tau_{0,0}^- < \tau_{0,0}^+ < \tau_{0,1}^- < \tau_{0,1}^+ < \dots < \tau_{0,9}^- < \tau_{0,9}^+ < \tau_{0,10}^- < \tau_{0,11}^- < \tau_{0,10}^+.$$

**Table 2.** Fitting parameters of system (2).

| Par. | Values | Par. | Values | Par. | Values | Par. | Values | Par. | Values |
|---|---|---|---|---|---|---|---|---|---|
| $a$ | 0.65 | $K$ | 25.0 | $b$ | 0.52 | $c$ | 0.009 | $d$ | 0.1 |
| $p_1$ | 0.11 | $p_2$ | 0.5 | $m$ | 0.25 | $q$ | 0.2 | $\alpha$ | 0.95 |

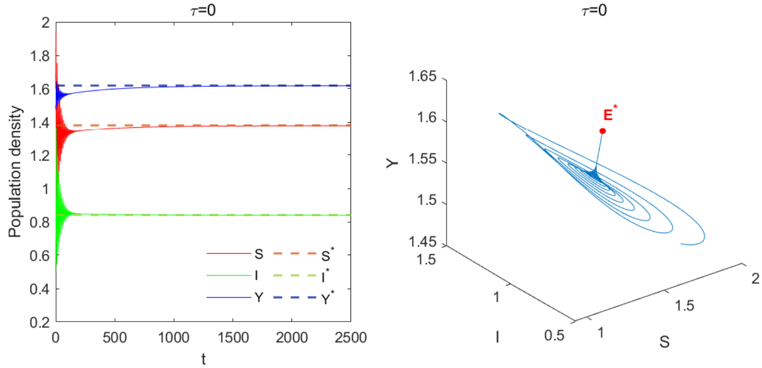


**Figure 1.** Solutions for system (2) with $\alpha = 0.95$ and $\tau = 0$.

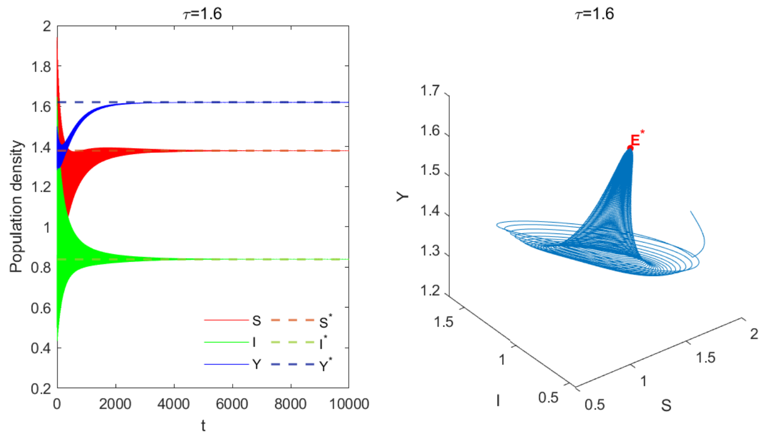


**Figure 2.** Solutions for system (2) with $\tau = 1.6$.

According to Theorem 2, the equilibrium $E^*$ is stable for $\tau$ within the intervals $[0, \tau_{0,0}^-)$, $(\tau_{0,k}^+, \tau_{0,k+1}^-)$ for $k = 0, 1, \dots, 9$, and unstable in the intervals $(\tau_{0,k}^-, \tau_{0,k}^+)$ with $k = 0, 1, \dots, 9$ and $(\tau_{1,10}^-, +\infty)$. Furthermore, system (2) undergoes a Hopf bifurcation at $E^*$ when $\tau = \tau_{0,k}^{\pm}$ for $k = 0, 1, \dots, 9$ and $\tau = \tau_{0,10}^-$. This alternating pattern of stability switches is illustrated in Figs. 2 and 3 for two cases: $E^*$ is locally asymptotically stable with $\tau = 1.6 \in (0, \tau_{0,0}^-)$, while it becomes unstable with $\tau = 2.5 \in (\tau_{0,0}^-, \tau_{0,0}^+)$.

To visualize the effect of the time delay $\tau$ on the dynamics of the infected prey, we numerically compute the bifurcation diagram shown in Fig. 4. The black horizontal

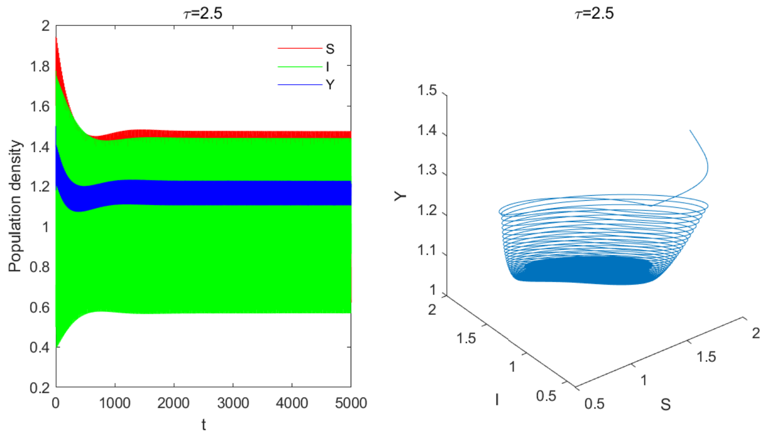


**Figure 3.** Solutions for system (2) with $\tau = 2.5$.

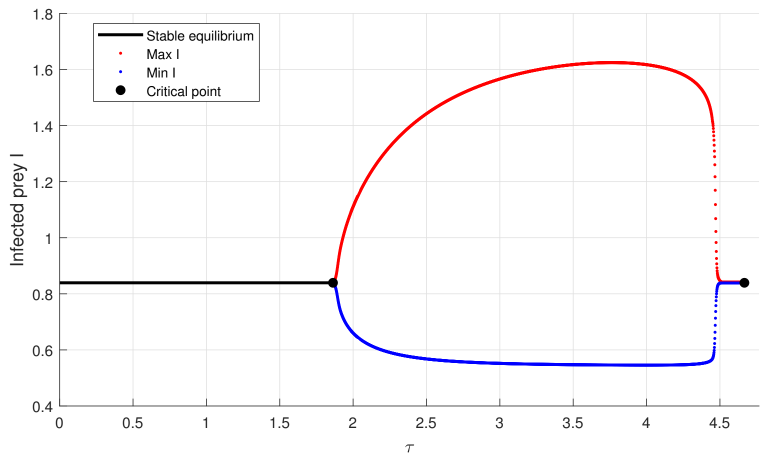


**Figure 4.** Bifurcation diagram of infected prey $I$ with respect to $\tau$.

line represents the stable equilibrium level $I^* = 0.8393$. The red dots denote the local maxima and the blue dots the local minima of the oscillatory solutions obtained by direct simulation for different $\tau$ values. For $\tau$ values between $\tau_{0,0}^- = 1.8628$ and $\tau_{0,0}^+ = 4.6668$, the system exhibits periodic oscillations. For brevity, we present only the first two bifurcating branches in this figure.

## 4.2 Control via delayed feedback

We now consider the controlled system (13) with the same parameter values as in the uncontrolled case, and the negative feedback gain is set to $h = -0.1$. With fixed $\tau = 2.5$, two positive roots $\psi_0^- \approx 0.5659$ and $\psi_0^+ \approx 0.604117$ are computed from Eq. (15). The

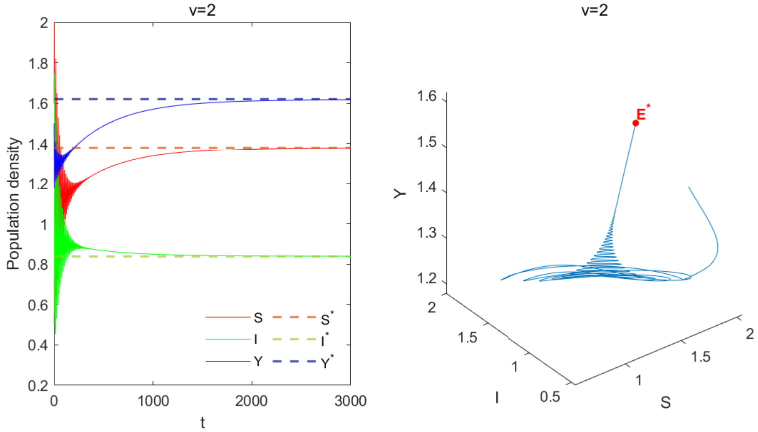


**Figure 5.** Solutions of system (13) with fixed $\tau = 2.5$ and $v = 2$.

corresponding fundamental critical delays, computed from (16), are

$$v_{0,k}^{\pm} = v_{0,0}^{\pm} + \frac{2k\pi}{\psi_0^{\pm}}, \quad k = 0, 1, 2, \ldots$$

with the fundamental critical delays $v_{0,0}^{-} \approx 0.6944$ and $v_{0,0}^{+} \approx 9.6919$, respectively. We have $U_1V_1+U_2V_2 \approx 0.0555 > 0$ for $(\psi_0^{-}, v_{0,k}^{-})$, and we have $U_1V_1+U_2V_2 \approx -0.1966 < 0$ for $(\psi_0^{+}, v_{0,k}^{+})$. Hence,

$$\operatorname{Re}\left[\left(\frac{ds}{dv}\right)^{-1}\right]_{v=v_{0,k}^{-}} < 0 \quad \text{and} \quad \operatorname{Re}\left[\left(\frac{ds}{dv}\right)^{-1}\right]_{v=v_{0,k}^{+}} > 0.$$

It is straightforward to verify that

$$0 < v_{0,0}^{-} < v_{0,0}^{+} < v_{0,1}^{-} < v_{0,1}^{+} < \cdots < v_{0,11}^{-} < v_{0,11}^{+} < v_{0,12}^{+} < v_{0,12}^{-}.$$

According to Theorem 3, the equilibrium $E^*$ is stable for $v$ within the intervals $(v_{0,k}^{-}, v_{0,k}^{+})$ with $k = 0, 1, \ldots, 11$, and unstable for $v$ in the complementary intervals, namely $[0, v_{0,0}^{-})$, $(v_{0,k}^{+}, v_{0,k+1}^{-})$ for $k = 0, 1, \ldots, 10$ and $(v_{0,11}^{+}, +\infty)$. Furthermore, system (13) undergoes a Hopf bifurcation at $E^*$ when $v = v_{0,k}^{\pm}$ for $k = 0, 1, \ldots, 11$. As shown in Fig. 5, stability at $E^*$ is restored for $\tau = 2.5$ by setting $v = 2$, which falls within the stabilizing interval $(v_{1,0}^{-}, v_{1,0}^{+})$.

### 4.3 Effect of fractional order $\alpha$

To quantitatively characterize the regulatory role of the fractional order $\alpha$ on the system dynamics, we determine the critical delay $\tau_0$ for Hopf bifurcation by solving the characteristic equation for different $\alpha$ values. It should be noted that the condition for the equilibrium to be stable at $\tau = 0$ is $|\arg(z_k)| > \alpha\pi/2$, where $z_k$ are the roots of the cubic

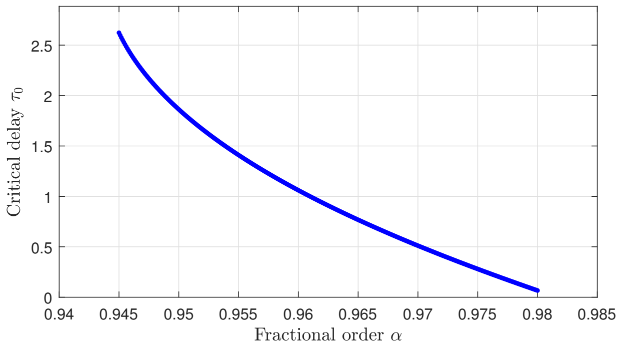


**Figure 6.** Hopf bifurcation threshold $\tau_0$ as a function of the fractional order $\alpha$.

equation (9). For the selected parameters, this condition requires $\alpha < \alpha_{\max} \approx 0.9816$; when $\alpha$ exceeds this threshold, the equilibrium is unstable even without delay. Therefore, we only consider $\alpha \leqslant 0.98$ to ensure a meaningful discussion of $\tau_0$.

According to the analysis in Section 3.2, substituting $s = \mathrm{i}\varphi$ ($\varphi > 0$) into the characteristic equation (10) yields the modulus condition $|Q_1(\mathrm{i}\varphi)| = |Q_2(\mathrm{i}\varphi)|$. Define the function $F(\varphi) = |Q_1(\mathrm{i}\varphi)| - |Q_2(\mathrm{i}\varphi)|$. Then a positive root of $F(\varphi) = 0$ corresponds to a frequency at which a Hopf bifurcation may occur. Numerical computations show that the modulus condition has no solution when $\alpha < 0.945$. In this case, the stability of the system does not change with $\tau$. Together with the fact that the equilibrium is stable at $\tau = 0$, we conclude that the system remains stable for all $\tau \geqslant 0$. This further confirms the stabilizing effect of strong memory, corresponding to small $\alpha$.

We numerically solve for the roots of $F(\varphi) = 0$ and compute the corresponding $\tau_0$ for each $\alpha$ in the range $[0.945, 0.98]$, with the results shown in Fig. 6. As $\alpha$ increases from $0.945$ to $0.98$, the critical delay $\tau_0$ decreases monotonically from about $2.62$ to about $0.067$. This indicates that a larger fractional order, which corresponds to a weaker memory effect, makes the system more sensitive to delay, meaning that the tolerable delay before destabilization becomes smaller. This provides intuitive numerical verification of the assertion in Remark 1 regarding the stabilizing role of memory and highlights the unique advantage of fractional-order modeling: by adjusting the memory strength, one can effectively suppress or delay harmful population oscillations.

## 5 Optimal control parameter design

In practical ecological management, control measures must strike a balance between effectiveness and cost. Excessive control may suppress disease transmission but lead to high implementation costs, while insufficient control fails to achieve the desired effect. To minimize the disease burden and control costs, we consider the following two objectives:

$$J_1(h, v) = \int_0^T I(t)\,\mathrm{d}t, \qquad J_2(h, v) = h^2,$$

which represent the cumulative number of infected individuals and the control cost, respectively. Thus, we construct the biobjective optimization problem

$$\min_{h,v}\bigl(J_1(h,v), J_2(h,v)\bigr) \quad \text{subject to dynamics of system (13).}$$

Here $h \in [-0.5, 0]$, $v \in [0.1, 10]$. To convert the biobjective problem into a single-objective one, we use the linear weighting method. Let $w_1, w_2 > 0$ with $w_1 + w_2 = 1$ be the weights for infection burden and control cost, respectively. The weighted objective function is defined as

$$J(h,v) = w_1 J_1(h,v) + w_2 J_2(h,v),$$

and the original problem becomes

$$\min_{h\in[-0.5,0],\, v\in[0.1,10]} J(h,v) \quad \text{subject to the dynamics of system (13).}$$

### 5.1 Optimization method

In the multicriteria decision-making framework, we set the objective function weights as $w_1 = 0.7$ and $w_2 = 0.3$ to balance the trade-off between infection scale and control cost. Since $J(h,v)$ lacks an explicit analytical form, we employ the pattern search algorithm [1] for derivative-free optimization. For each $(h,v)$, $J(h,v)$ is obtained by numerically solving system (13) and integrating $I(t)$. The optimization is set with a maximum of 20 iterations and a function tolerance of $10^{-4}$, ensuring convergence while maintaining computational efficiency.

Figure 7(a) shows the convergence process of the pattern search algorithm. The objective function value steadily decreases from an initial value of 1200.62, reaching the

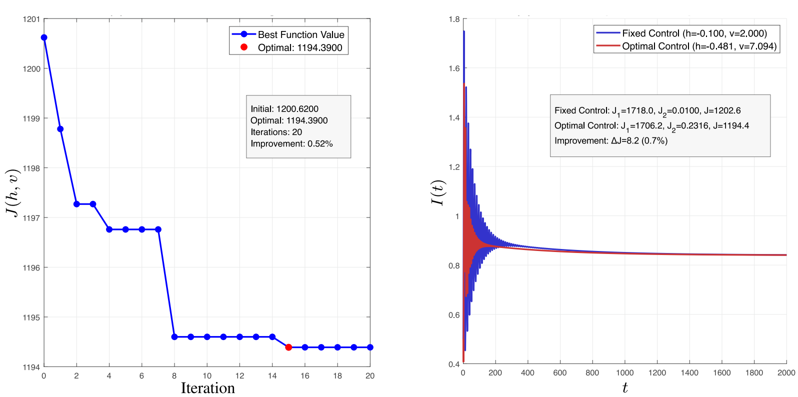


(a) Pattern search convergence (b) Infected population comparison

**Figure 7.** (a) Convergence process of pattern search: the objective function value converges to 1194.39 after 15 iterations; (b) Comparison of infected individuals: the optimized control strategy significantly reduces the cumulative infection scale.

optimal value of $1194.39$ at the 15th iteration and remaining unchanged in subsequent iterations, indicating algorithm convergence. The algorithm finally obtains the optimal parameters $h^* = -0.481$, $v^* = 7.094$. The corresponding optimal objective function value is $J^* = 1194.39$, with cumulative infection scale $J_1^* = 1706.17$ and control cost $J_2^* = 0.2316$.

To evaluate the effectiveness of the optimized control strategy, we compare it with a fixed control strategy $h = -0.1$, $v = 2$. Figure 7(b) shows that the infected individual curve $I(t)$ under the optimized control strategy is always below that of the fixed control strategy, indicating its superiority in suppressing epidemic spread. From a cost perspective, the optimized strategy reduces the total objective function value $J$ by $0.7\%$.

It is worth noting that although the control cost $J_2$ of the optimized strategy increases significantly due to stronger feedback, the cumulative infection scale $J_1$ decreases more substantially, achieving overall cost optimization. This result suggests that moderately strengthening intervention intensity in infectious disease control can bring greater social benefits by reducing the infection scale.

### 5.2 Weight sensitivity analysis

To assess how decision-maker preferences affect the optimal strategy and model robustness, we perform a sensitivity analysis on the weight $w_1$. The biobjective problem is transformed into the following single-objective optimization problem via the linear weighting method:

$$\min J(x) = w_1 J_1(x) + (1 - w_1) J_2(x), \quad x = [h, v]^\top.$$

For each $w_1 \in \{0, 0.1, 0.2, \ldots, 1.0\}$, the above optimization problem is solved using the pattern search algorithm, and the optimal solution $(h^*, v^*)$ along with the corresponding objective values $(J_1^*, J_2^*)$ are recorded. By analyzing the trend of the optimal solution as $w_1$ varies, we assess the sensitivity and robustness of the model. The sensitivity analysis results are shown in Table 3.

It is observed that when $w_1 < 0.4$, $h^*$ and $v^*$ change significantly; when $w_1 \geqslant 0.4$, both tend to stabilize. These results indicate that the model is insensitive to preference

**Table 3.** Optimal strategies and objective values under different weight coefficients.

| $w_1$ | Decision variables | | Objective values | | $J^*$ |
|---|---|---|---|---|---|
| | $h^*$ | $v^*$ | $J_1^*$ | $J_2^*$ | |
| 0.00 | −0.0047 | 2.0000 | 1860.68 | 0.0000 | 0.00 |
| 0.10 | −0.2547 | 7.0000 | 1708.86 | 0.0649 | 170.94 |
| 0.20 | −0.4422 | 7.0000 | 1706.57 | 0.1955 | 341.47 |
| 0.30 | −0.4891 | 7.0625 | 1706.09 | 0.2392 | 512.00 |
| 0.40 | −0.4969 | 7.0781 | 1706.02 | 0.2469 | 682.56 |
| 0.50 | −0.4988 | 7.0859 | 1706.00 | 0.2488 | 853.13 |
| 0.60 | −0.4988 | 7.0625 | 1706.00 | 0.2488 | 1023.70 |
| 0.70 | −0.4998 | 7.0664 | 1705.99 | 0.2498 | 1194.27 |
| 0.80 | −0.4998 | 7.0664 | 1705.99 | 0.2498 | 1364.84 |
| 0.90 | −0.4998 | 7.0664 | 1705.99 | 0.2498 | 1535.42 |
| 1.00 | −0.4998 | 7.0664 | 1705.99 | 0.2498 | 1705.99 |

changes when the weight $w_1 \geqslant 0.4$. The optimal strategy remains stable as long as infection control is assigned at least 40%. In contrast, the system is more sensitive to weight changes in the range $w_1 < 0.4$, which requires a nuanced balance between infection control and cost considerations.

### 5.3 Biological interpretation

The sensitivity analysis reveals a critical decision inflection point at $w_1 = 0.4$. When the preference weight exceeds this value, further increases yield diminishing returns in reducing infections, with minimal changes to the optimal strategy. For $w_1 \in [0.4, 1.0]$, the optimal control parameters are $h^* \approx -0.5$ and $v^* \approx 7.1$ days, the resulting cumulative infections are $J_1^* \approx 1706$. This stability indicates that the recommended strategy is robust as long as infection control is prioritized with at least $40\%$ weight. In contrast, when resources are limited and control effectiveness must be carefully balanced against cost, the focus should be on the more sensitive interval $w_1 \in [0.2, 0.4]$. Within this range, small adjustments in the weight coefficient lead to substantial variations in both the optimal strategy and outcomes, making it the critical interval for policy adjustment.

## 6 Conclusions

We analyze a fractional-order eco-epidemiological predator–prey model with time delay and Holling type II response. We first determine all possible equilibria and analyze their stability. For the uncontrolled system, we derive explicit stability conditions for the positive equilibrium $E^*$ in the absence of delay. When $\tau$ exceeds $\tau_0$, a Hopf bifurcation occurs, generating periodic oscillations. Figure 4 shows the bifurcation diagram, and Fig. 6 shows that $\tau_0$ decreases as $\alpha$ increases, confirming that stronger memory effects enhance stability.

To control disease outbreaks, we introduce a delayed feedback controller $\mu(t) = h[I(t) - I(t-v)]$ into the infected prey equation. This controller delays the Hopf bifurcation and stabilizes the system under certain conditions. We derive critical $v$ values and verify via simulations that the controller can suppress or induce stability depending on $v$.

Numerical simulations confirm the theory, showing stability loss as $\tau$ increases and recovery via fractional-order reduction or delayed feedback. A biobjective optimization (Section 5) yields $(h^*, v^*) = (-0.481, 7.094)$ via pattern search. Sensitivity analysis shows the optimal strategy is robust when infection control weighting $\geqslant 40\%$, while $[0.2, 0.4]$ requires fine-tuning.

Limitations include the specific Holling type II response and linear feedback, which may not capture ratio-dependent predation, nonlinear costs, or stochastic fluctuations. The analysis is local, leaving global dynamics and multidelay interactions for future work.

Future directions: (i) generalized functional responses; (ii) adaptive or real-time control; (iii) age/stage structure, stochastic perturbations, or spatial diffusion. Such extensions would bridge theory and real-world dynamics, enhancing applicability for conservation and public health.

**Author contributions.** The authors (W.Z. and J.Z.) have contributed as follows: methodology, W.Z.; formal analysis, W.Z. and J.Z.; validation, W.Z.; writing – original draft preparation, W.Z.; writing – review & editing, W.Z. and J.Z. Both authors have read and approved the published version of the manuscript.

**Conflicts of interest.** The authors declare no conflicts of interest.

## References


1. C. Audet, J.E. Dennis, Jr., Analysis of generalized pattern searches, *SIAM J. Optim.*, **13**(3):889–903, 2002, `https://doi.org/10.1137/S1052623400378742`.
2. P. Auger, R. Mchich, T. Chowdhury, G. Sallet, M. Tchuente, J. Chattopadhyay, Effects of a disease affecting a predator on the dynamics of a predator–prey system, *J. Theor. Biol.*, **258**:344–351, 2009, `https://doi.org/10.1016/j.jtbi.2008.10.030`.
3. J. Chattopadhyay, O. Arino, A predator-prey model with disease in the prey, *Nonlinear Anal., Theory Methods Appl.*, **36**:747–766, 1999, `https://doi.org/10.1016/S0362-546X(98)00126-6`.
4. K. Diethelm, A fractional calculus based model for the simulation of an outbreak of dengue fever, *Nonlinear Dyn.*, **74**(4):613–619, 2013, `https://doi.org/10.1007/s11071-012-0475-2`.
5. G.-P. Hu, X.-L. Li, Stability and Hopf bifurcation for a delayed predator–prey model with disease in the prey, *Chaos Solitons Fractals*, **45**(3):229–237, 2012, `https://doi.org/10.1016/j.chaos.2011.11.011`.
6. Y. Jalilian, R. Jalilian, Existence of solution for delay fractional differential equations, *Mediterr. J. Math.*, **10**(4):1731–1747, 2013, `https://doi.org/10.1007/s00009-013-0281-1`.
7. A. Kumar, S. Kumar, A study on eco-epidemiological model with fractional operators, *Chaos Solitons Fractals*, **156**:111697, 2022, `https://doi.org/10.1016/j.chaos.2021.111697`.
8. N. Liu, J. Wang, Q. Lan, W. Deng, Dynamics and event-triggered impulsive control of a fractional-order epidemic model with time delay, *Fractal Fract.*, **8**(1):22, 2024, `https://doi.org/10.3390/fractalfract8010022`.
9. W. Ma, M. Song, Y. Takeuchi, Global stability of an sir epidemic model with time delay, *Appl. Math. Lett.*, **17**(10):1141–1145, 2004, `https://doi.org/10.1016/j.aml.2003.11.005`.
10. N.M. Oliveira, F.M. Hilker, Modelling disease introduction as biological control of invasive predators to preserve endangered prey, *Bull. Math. Biol.*, **72**:444–468, 2010, `https://doi.org/10.1007/s11538-009-9454-2`.
11. H.S. Panigoro, N. Anggriani, E. Rahmi, Understanding the role of intraspecific disease transmission and quarantine on the dynamics of eco-epidemiological fractional order model, *Fractal Fract.*, **7**:610, 2023, `https://doi.org/10.3390/fractalfract7080610`.
12. I. Petráš, *Fractional-Order Nonlinear Systems: Modeling, Analysis and Simulation*, Nonlinear Phys. Sci., Springer, Berlin, Heidelberg, 2011, `https://doi.org/10.1007/978-3-642-18101-6`.

13. R.K. Plowright, A.N. Ahmed, et all., Ecological countermeasures to prevent pathogen spillover and subsequent pandemics, *Nat. Commun.*, **15**:2577, 2024, `https://doi.org/10.1038/s41467-024-46151-9`.
14. H. Qi, W. Zhao, Stability and bifurcation control analysis of a delayed fractional-order eco-epidemiological system, *Eur. Phys. J. Plus*, **137**:934, 2022, `https://doi.org/10.1140/epjp/s13360-022-03154-z`.
15. G. She, F. Yi, Dynamics and bifurcations in a nondegenerate homogeneous diffusive SIR rabies model, *SIAM J. Appl. Math.*, **84**(2):632–660, 2024, `https://doi.org/10.1137/23M159055X`.
16. A.A. Thirthar, N. Sk, B. Mondal, M.A. Alqudah, T. Abdeljawad, Utilizing memory effects to enhance resilience in disease-driven prey-predator systems under global warming, *J. Appl. Math. Comput.*, **69**:4617–4643, 2023, `https://doi.org/10.1007/s12190-023-01936-x`.
17. Q. Wang, R. Han, Dynamics of fractional-order predator prey models with refuge and Allee effect in prey: With and without time delay, *Qual. Theory Dyn. Syst.*, **24**:49, 2025, `https://doi.org/10.1007/s12346-024-01212-8`.
18. X. Wang, Z. Wang, J. Xia, Stability and bifurcation control of a delayed fractional-order eco-epidemiological model with incommensurate orders, *J. Franklin Inst.*, **356**(15):8278–8295, 2019, `https://doi.org/10.1016/j.jfranklin.2019.07.028`.
19. Z. Wu, Y. Cai, Z. Wang, W. Wang, Global stability of a fractional order SIS epidemic model, *J. Differ. Equations*, **352**:221–248, 2023, `https://doi.org/10.1016/j.jde.2022.12.045`.
20. M. Xiao, G. Jiang, J. Cao, W. Zheng, Local bifurcation analysis of a delayed fractional-order dynamic model of dual congestion control algorithms, *IEEE/CAA J. Autom. Sin.*, **4**(2):361–369, 2017, `https://doi.org/10.1109/JAS.2016.7510151`.
21. Y. Xiao, L. Chen, Modeling and analysis of a predator–prey model with disease in the prey, *Math. Biosci.*, **171**(1):59–82, 2001, `https://doi.org/10.1016/S0025-5564(01)00049-9`.
22. C. Xu, Y. Yu, Y. Chen, Z. Lu, Forecast analysis of the epidemics trend of COVID-19 in the USA by a generalized fractional-order SEIR model, *Nonlinear Dyn.*, **101**(3):1621–1634, 2020, `https://doi.org/10.1007/s11071-020-05946-3`.
23. C. Xu, Y. Yu, G. Ren, X. Si, Optimal control and bifurcation analysis of a delayed fractional-order SIRS model with general incidence rate and delayed control, *Nonlinear Anal. Model. Control*, **29**(5):890–913, 2024, `https://doi.org/10.15388/namc.2024.29.35789`.
24. S. Xu, Y. Hu, Dynamic analysis of a Caputo fractional-order SEIR model with a general incidence rate, *Sci. Rep.*, **15**:17561, 2025, `https://doi.org/10.1038/s41598-025-01400-9`.
25. F. Yi, J. Wei, J. Shi, Bifurcation and spatiotemporal patterns in a homogeneous diffusive predator–prey system, *J. Differ. Equations*, **246**:1944–1977, 2009, `https://doi.org/10.1016/j.jde.2008.10.024`.
26. J. Zeng, X. Chen, L. Wei, D. Li, Bifurcation analysis of a fractional-order eco-epidemiological system with two delays, *Nonlinear Dyn.*, **112**:22505–22527, 2024, `https://doi.org/10.1007/s11071-024-10184-y`.

27. X. Zhang, Q. Yang, T. Su, Dynamical behavior and numerical simulation of a stochastic eco-epidemiological model with Ornstein–Uhlenbeck process, *Commun. Nonlinear Sci. Numer. Simul.*, **123**:107284, 2023, https://doi.org/10.1016/j.cnsns.2023.107284.
28. X. Zhou, J. Cui, Stability and Hopf bifurcation of a delay eco-epidemiological model with nonlinear incidence rate, *Math. Model. Anal.*, **15**(4):547–569, 2010, https://doi.org/10.3846/1392-6292.2010.15.547-569.